JACS
JOURNAL OF THE AMERICAN CHEMICAL SOCIETY
Communication
pubs.acs.org/JACS

Partitioning MOF-5 into Confined and Hydrophobic Compartments for Carbon Capture under Humid Conditions

Nan Ding,[†] Haiwei Li,[†] Xiao Feng,* Qianyou Wang, Shan Wang, Li Ma, Junwen Zhou, and Bo Wang*

Key Laboratory of Cluster Science, Ministry of Education of China, School of Chemistry, Beijing Institute of Technology, 5 South Zhongguancun Street, Beijing 100081, P. R. China

Supporting Information

ABSTRACT: Metal−organic frameworks (MOFs), by virtue of their remarkable uptake capability, selectivity, and ease of regeneration, hold great promise for carbon capture from fossil fuel combustion. However, their stability toward moisture together with the competitive adsorption of water against CO_2 drastically dampens their capacity and selectivity under real humid flue gas conditions. In this work, an effective strategy was developed to tackle the above obstacles by partitioning the channels of MOFs into confined, hydrophobic compartments by in situ polymerization of aromatic acetylenes. Specifically, polynaphthylene was formed via a radical reaction inside the channels of MOF-5 and served as partitions without altering the underlying structure of the framework. Compared with pristine MOF-5, the resultant material (PN@MOF-5) exhibits a doubled CO_2 capacity (78 vs 38 cm^3/g at 273 K and 1 bar), 23 times higher CO_2/N_2 selectivity (212 vs 9), and significantly improved moisture stability. The dynamic CO_2 adsorption capacity can be largely maintained (>90%) under humid conditions during cycles. This strategy can be applied to other MOF materials and may shed light on the design of new MOF−polymer materials with tunable pore sizes and environments to promote their practical applications.

Fossil fuel combustion from stationary sources makes up the majority of the total anthropogenic CO_2 contributions, raising huge environmental challenges facing our planet.[1] Although aqueous alkanolamine solutions are the state-of-the-art capture absorbents that have been broadly implemented in power plants for CO_2 capture, their regeneration from carbamates inevitably leads to a huge energy penalty.[2] Metal−organic frameworks (MOFs), constructed from organic linkers and metal ions or clusters, represent one of the most promising materials for CO_2 capture and storage.[2c,3] Because of their high porosities, structural diversity, tunable pore environments, and atomically well-defined skeletons, MOFs have been extensively explored in various applications, such as gas storage and separation, catalysis, and chemosensing.[4]

Increasing MOF surface area and pore size is one of the most efficient approaches to maximize CO_2 uptake and can dramatically enhance the storage capacity under high pressure (>3−5 MPa).[5] However, such high adsorption is often not viable when MOFs are used in power plants postcombustion, where the pressure of the flue gas from smoke stacks is usually below 0.3 MPa.[6] Indeed, pore surface functionalization of MOFs is the most widely used method for the efficient and selective carbon capture. Generally, functional groups with high polarity, such as pyridine, −OH, $-NO_2$, −CN, −SH, etc., and/or open metal sites decorating the walls of MOF pores are favorable, since CO_2 molecules possess a large quadrupole moment and these functional sites are able to induce polarization and enhance the affinity.[3a,b,7] Another effective way to improve the CO_2 capacity and selectivity is to anchor basic amine groups onto the MOF skeleton to mimic the chemisorption in liquid absorbents.[8] Nevertheless, aside from ∼75% N_2 and ∼15% CO_2, a typical postcombustion flue gas also contains 5−7% water, which must be thoroughly taken into consideration for real applications.[2c,3a,b,9] During the separation process, water molecules, which have higher polarity and binding energy, will strongly compete against CO_2, and therefore, the active adsorption sites in MOFs are easily poisoned by only small amount of water. Consequently, the capacity and selectivity are dramatically dampened under real humid flue gas conditions.[10]

Needless to say, many MOF structures are vulnerable under moist conditions, and the collapse of the framework by slow hydrolysis can significantly lower the separation performance and impede their practical application.[10c,11] Alternatively, trapping of CO_2 in a confined space offers opportunities to separate gas molecules on the basis of size. Because of the difficulties in designing and synthesizing MOFs with pore openings that exactly match the kinetic diameter of the CO_2 molecule, only few pioneering works have been reported.[12] Therefore, the demand for a facile method to prepare moisture-stable MOF materials that can selectively adsorb CO_2 over other gas components and water molecules from flue gas is ever urgent yet largely unmet.

Recently, Cohen and co-workers reported polymer−metal−organic frameworks that can selectively adsorb CO_2 over N_2 and exhibit high water stability.[13] Kitagawa and co-workers have pioneered in situ polymerization of vinyl monomers inside the channels of MOFs.[14] Inspired by their works, herein we report a strategy that can divide the open channels of MOFs into confined and hydrophobic compartments by in situ polymerization of aromatic acetylenes inside MOF pores. The thus-obtained MOF material can capture and trap CO_2 molecules and effectively retard the diffusion and repel water molecules. We intentionally selected MOF-5, a famous and highly porous

Received: June 13, 2016
Published: August 1, 2016

DOI: 10.1021/jacs.6b06051
J. Am. Chem. Soc. 2016, 138, 10100−10103

MOF structure that can also be produced on an industrial scale (>1 ton per 30 min),[15] to serve as the prototype host material. 1,2-Diethynylbenzene (DEB) as the monomer was adsorbed and encapsulated in MOF-5 and further heated at elevated temperature to afford polynaphthylene (PN) inside the channels via Bergman cyclization and subsequent radical polymerization (Scheme 1). The resulting composite is

Scheme 1. (a) Illustration of Competitive Adsorption of CO_2 against H_2O at the Surface and Edge of PN; (b) Polymerization of DEB in MOFs

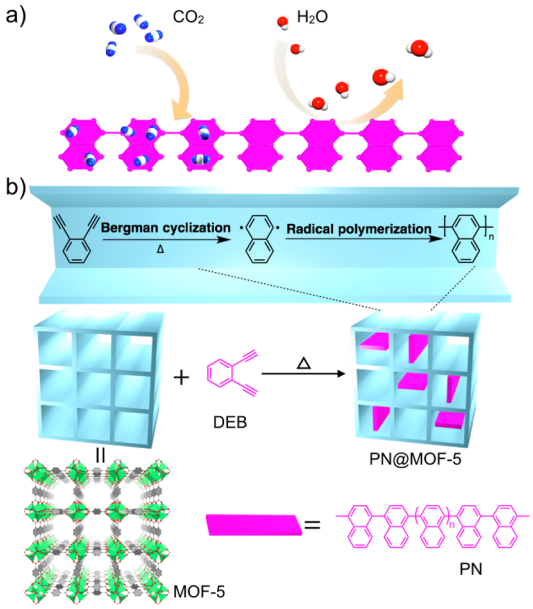

denoted as PN@MOF-5. Because of its hydrophobic and linear nature, PN in MOF-5 can act as partitions to segregate the micropores (with widths of ~1.2 nm) into ultra-micropores (≤0.7 nm) and simultaneously improve the stability of PN@MOF-5 toward moisture.

In contrast to MOF-5, which is water-sensitive, PN@MOF-5 can retain its crystallinity and porosity upon exposure to humid air (>40 h, relative humidity (RH) = 40%). More importantly, the ultra-micropores and large number of exposed of aromatic edges and surfaces in PN@MOF-5 allow it to capture CO_2 efficiently (Scheme 1). Compared with pristine MOF-5, the thermodynamic adsorption capacity of CO_2 is doubled and the CO_2/N_2 selectivity (in 14:86 CO_2/N_2 at 1 bar and 273 K) is increased 23-fold for PN@MOF-5. Furthermore, in breakthrough experiments, PN@MOF-5 largely maintained its dynamic CO_2 capacity under humid conditions (>90% retention rate at RH = 65%).

The details of the polymerization of DEB in MOF-5 are described in the Supporting Information. A significant color change from white to brown was observed after heating (Figures S3 and S4), indicative of the formation of highly conjugated polymers. The powder X-ray diffraction (PXRD) pattern of PN@MOF-5 is consistent with that of MOF-5 (Figure S5), indicating that the crystalline structure is retained during inclusion and polymerization of DEB. ^{13}C solid-state NMR spectra of PN@MOF-5 as well as the PN polymer isolated from PN@MOF-5 (Figure S7) display the signals of aromatic carbons belonging to the polynaphthylene at ~128 ppm. The disappearance of the C≡C−H stretching vibration at 3300 cm^{-1} and the C≡C−H bending vibration at ~700 cm^{-1} in the Fourier transform infrared attenuated total reflection (FTIR-ATR) spectrum of PN@MOF-5 (Figure S8) reflects the high degree of polymerization of acetylene. As determined by elemental analysis, the loading of PN in the host−polymer inclusion is 15.0 wt % (Table S1). The PN loading can be adjusted by carefully altering the amount of solvent used for washing before polymerization, and accordingly, another three inclusion samples with PN loadings of 3.2, 34, and 40 wt % (denoted as PN_x@MOF-5, where x is the wt % loading) were obtained. Scanning electron microscopy (SEM) and optical microscopy images of the two PN@MOF-5 samples (Figures S9 and S10) display their preserved crystal morphologies. To address whether the PN polymers homogeneously existed in large domains (greater than a nanometer scale), each crystal was dissected into two segments. The color was almost evenly distributed in each crystal, and a higher loading amount resulted in a deeper color.

Nitrogen sorption isotherm tests at 77 K were conducted to access their porosities. Analyses of the sorption curves of MOF-5, $PN_{3.2}$@MOF-5, and PN@MOF-5 (Figure S11) by the Brunauer−Emmett−Teller (BET) method gave specific surface areas of 3200, 2600, and 1200 $m^2\ g^{-1}$, respectively (Figures S12−S14). Quenched solid-state density functional theory (QSDFT) was utilized to deduce the pore size distributions (Figure 1a). Interestingly, with increasing PN loading, the pores

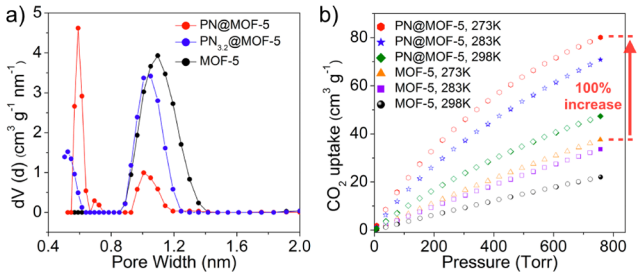

Figure 1. (a) Pore size distributions of PN@MOF-5, $PN_{3.2}$@MOF-5, and MOF-5 based on quenched solid-state density functional theory. (b) CO_2 sorption isotherms of PN@MOF-5 and MOF-5 at 273, 283, and 298 K.

with widths of 1.2 nm (MOF-5 pores) gradually diminish, whereas pores with widths of 0.6 nm (partitioned pores) emerge and are boosted significantly. These results demonstrate that the PN polymers can act as partitions to segregate the channels of the crystals into confined compartments. Although these analyses do not preclude the presence of PN polymers wrapping the surface of the crystals, we believe that the overall consideration of the pore size distribution analysis, PXRD measurements, and microscopy images strongly supports that most of the PN polymers are distributed inside the crystal channels and serve as partitions.

Compartments with confined space together with abundant exposed surfaces and edges of aromatic rings in PN@MOF-5 are supposed to be favorable for CO_2 capture.[16] Considering a balance between partitioning and partial blocking of the MOF channels (Figures S15 and S16), we selected PN@MOF-5 to perform CO_2 sorption isotherm tests at different temperatures and calculated its adsorption enthalpy. Remarkably, compared with MOF-5 (38 $cm^3\ g^{-1}$ at 273 K and 760 Torr), a doubled CO_2 capacity of PN@MOF-5 (78 $cm^3\ g^{-1}$ at 273 K and 760 Torr; Figure 1b) with just one-third of the BET surface area of

DOI: 10.1021/jacs.6b06051
J. Am. Chem. Soc. 2016, 138, 10100−10103

MOF-5 is achieved. It is worth noting that the pore size distribution derived from the CO_2 adsorption isotherm at 273 K using the nonlocal DFT (NLDFT) method (Figure S17) displays a maximum at about 0.5−0.6 nm as well as partial pores at 0.37 and 0.81 nm. We further employed the Clausius−Clapeyron formula to determine the isosteric heats of adsorption (Q_{st}) from CO_2 adsorption isotherms at 273, 283, and 298 K (Figures 1b and S18). At zero loading the Q_{st} value ($-\Delta H$) is 29 kJ/mol, and at higher loadings it decreases to ~24 kJ/mol, which is still one-third higher than that of MOF-5. The fact that twice the amount of CO_2 is adsorbed in the comparatively low-surface-area material of PN@MOF-5 with a larger Q_{st} can be attributed to the enhanced adsorbate−surface interactions with both sides or ends of the CO_2 molecules stemming from the confined pore size effect and the greater number of exposed aromatic surfaces.

Ideal adsorption solution theory (IAST) was applied in order to predict the expected selectivity for CO_2 over N_2 for the materials (Figure 3a). Under simulated postcombustion flue gas composition (14% CO_2, 86% N_2), the calculated CO_2/N_2 selectivity at 1 bar and 273 K for PN@MOF-5 (212) is almost 23 times higher than that of MOF-5 (9) (Table S2).

MOF-5 is very sensitive to moisture as a result of breakdown of the coordination bonds by the attack of water molecules.[17] In contrast to the hydrophilic nature of MOF-5 with a water contact angle close to 0°, PN@MOF-5 is hydrophobic and exhibits a water contact angle of 135° (Figure 2a). MOF-5

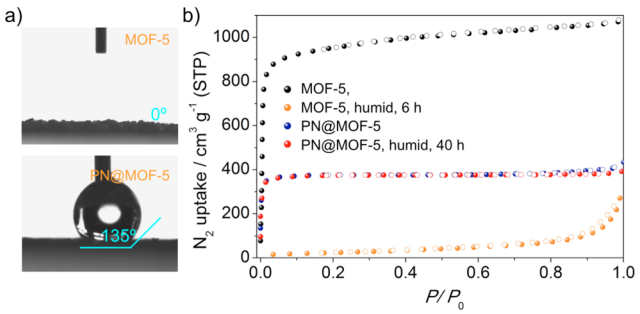

Figure 2. (a) Contact angle measurements. (b) Nitrogen sorption profiles of PN@MOF-5 and MOF-5 after exposure to humidity for different times.

completely loses its porosity within 6 h and is transformed into MOF-69c[18] within 40 h in a humid environment (RH = 40%), as evidenced by PXRD and N_2 sorption isotherm measurements (Figures 2b and S23). On the contrary, the BET surface area and crystallinity of PN@MOF-5 are preserved after moisture treatment for 40 h (Figures 2b and S23), indicating that the inclusion of aromatic PN into the channels can effectively prevent the attack on the coordination bonds by water. Similar results were observed for $PN_{3.2}$@MOF-5 (Figures S24 and S25).

Given the high humidity stability, hydrophobicity, and good CO_2 uptake capacity, we carried out dynamic separation experiments to test the ability of PN@MOF-5 to separate CO_2 from N_2 with and without moisture (details are provided in Figure S26). A N_2/CO_2 gas mixture with 16% CO_2 content was introduced to the bed, and the effluent was monitored by a mass spectrometer (Figure 3b,c). Under dry conditions, the PN@MOF-5 adsorbent bed showed a dynamic CO_2 adsorption capacity of 34 cm^3/g, which is 1.5 times that of MOF-5 prepared under similar conditions (23 cm^3/g). For the humid

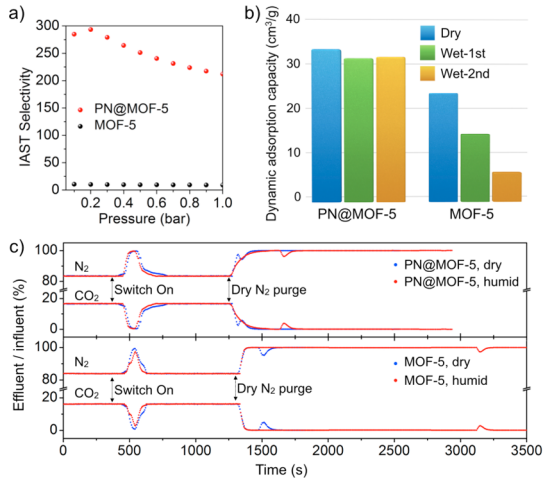

Figure 3. (a) Calculated IAST selectivity for CO_2 over N_2 at 273 K for a 14:86 CO_2/N_2 gas mixture. (b) Capacities and (c) dynamic sorption curves of PN@MOF-5 and MOF-5 under dry conditions (blue) and in the presence of water (red).

conditions test, a gas mixture (84:16 v/v N_2/CO_2) was introduced to the bed at RH = 65%. The dynamic sorption capacity of PN@MOF-5 under moisture was almost the same as the value obtained under dry conditions, while MOF-5 displayed decreases of 40% and 73% in the first and second cycles, respectively, in the presence of water (Figure 3b,c). In addition, the topology of PN@MOF-5 remained intact after dynamic sorption, while the skeleton of MOF-5 was almost collapsed (Figure S29). For comparison, the two representative MOFs MOF-199 and NH_2-UiO-66 significantly lost their CO_2 capacity under humid conditions (Table S3).

In conclusion, we have reported a new strategy to divide MOF pores into confined compartments by in situ polymerization of aromatic acetylene. For PN@MOF-5, a remarkable increase in CO_2 adsorption capacity from 38 to 78 cm^3/g and in CO_2/N_2 selectivity from 9 to 212 at 273 K and 1 bar were obtained. As a result of its hydrophobic nature, not only was the stability of the framework toward moisture significantly improved, but also, the competitive adsorption of water against CO_2 was effectively inhibited. Consequently, the dynamic CO_2 capacity under humid conditions reached a 94% retention rate. The improved stability toward moisture and increased adsorption capacity of PN@UMCM-8 (Figures S32−S34) demonstrate the applicability of the present strategy. The abundant combinations of porous materials (i.e., MOFs, covalent organic frameworks,[19] porous polymers, etc.) and conventional polymers will provide versatile material platforms for achieving multiple functions and practical applications.

■ ASSOCIATED CONTENT

Supporting Information

The Supporting Information is available free of charge on the ACS Publications website at DOI: 10.1021/jacs.6b06051.

Experimental details and additional data (PDF)

■ AUTHOR INFORMATION

Corresponding Authors

*bowang@bit.edu.cn

*fengxiao86@bit.edu.cn;

DOI: 10.1021/jacs.6b06051
J. Am. Chem. Soc. 2016, 138, 10100−10103

Author Contributions

†N.D. and H.L. contributed equally.

Notes

The authors declare no competing financial interest.

■ ACKNOWLEDGMENTS

This work was financially supported by the 973 Program (2013CB834704), the National Natural Science Foundation of China (21471018, 21404010, 21201018, and 21490570), and the 1000 Plan (Youth).

■ REFERENCES

(1) Pachauri, R. K.; Reisinger, A. *Intergovernmental Panel on Climate Change*; IPCC Secretariat: Geneva, 2007.

(2) (a) Rochelle, G. T. *Science* **2009**, *325*, 1652. (b) Haszeldine, R. S. *Science* **2009**, *325*, 1647. (c) Schoedel, A.; Ji, Z.; Yaghi, O. M. *Nature Energy* **2016**, *1*, 16034.

(3) (a) Sumida, K.; Rogow, D. L.; Mason, J. A.; McDonald, T. M.; Bloch, E. D.; Herm, Z. R.; Bae, T. H.; Long, J. R. *Chem. Rev.* **2012**, *112*, 724. (b) Zhang, Z. J.; Yao, Z. Z.; Xiang, S. C.; Chen, B. L. *Energy Environ. Sci.* **2014**, *7*, 2868. (c) Li, J. R.; Ma, Y. G.; McCarthy, M. C.; Sculley, J.; Yu, J. M.; Jeong, H. K.; Balbuena, P. B.; Zhou, H. C. *Coord. Chem. Rev.* **2011**, *255*, 1791. (d) Sreenivasulu, B.; Sreedhar, I.; Suresh, P.; Raghavan, K. V. *Environ. Sci. Technol.* **2015**, *49*, 12641.

(4) (a) Li, H.; Eddaoudi, M.; O'Keeffe, M.; Yaghi, O. M. *Nature* **1999**, *402*, 276. (b) Kitaura, R.; Kitagawa, S.; Kubota, Y.; Kobayashi, T. C.; Kindo, K.; Mita, Y.; Matsuo, A.; Kobayashi, M.; Chang, H.-C.; Ozawa, T. C.; Suzuki, M.; Sakata, M.; Takata, M. *Science* **2002**, *298*, 2358. (c) Férey, G. *Chem. Soc. Rev.* **2008**, *37*, 191. (d) Li, J. R.; Kuppler, R. J.; Zhou, H. C. *Chem. Soc. Rev.* **2009**, *38*, 1477. (e) Yoon, M.; Srirambalaji, R.; Kim, K. *Chem. Rev.* **2012**, *112*, 1196. (f) Guo, Y. X.; Feng, X.; Han, T. Y.; Wang, S.; Lin, Z. G.; Dong, Y. P.; Wang, B. *J. Am. Chem. Soc.* **2014**, *136*, 15485. (g) Wang, L.; Feng, X.; Ren, L. T.; Piao, Q. H.; Zhong, J. Q.; Wang, Y. B.; Li, H. W.; Chen, Y. F.; Wang, B. *J. Am. Chem. Soc.* **2015**, *137*, 4920.

(5) (a) Millward, A. R.; Yaghi, O. M. *J. Am. Chem. Soc.* **2005**, *127*, 17998. (b) Farha, O. K.; Yazaydin, A. O.; Eryazici, I.; Malliakas, C. D.; Hauser, B. G.; Kanatzidis, M. G.; Nguyen, S. T.; Snurr, R. Q.; Hupp, J. T. *Nat. Chem.* **2010**, *2*, 944. (c) Furukawa, H.; Ko, N.; Go, Y. B.; Aratani, N.; Choi, S. B.; Choi, E.; Yazaydin, A. O.; Snurr, R. Q.; O'Keeffe, M.; Kim, J.; Yaghi, O. M. *Science* **2010**, *329*, 424.

(6) *Handbook of Clean Energy Systems*; Yan, J., Ed.; John Wiley & Sons: Chichester, U.K., 2015; Vol. 5.

(7) (a) Caskey, S. R.; Wong-Foy, A. G.; Matzger, A. J. *J. Am. Chem. Soc.* **2008**, *130*, 10870. (b) Li, B. Y.; Zhang, Z. J.; Li, Y.; Yao, K. X.; Zhu, Y. H.; Deng, Z. Y.; Yang, F.; Zhou, X. J.; Li, G. H.; Wu, H. H.; Nijem, N.; Chabal, Y. J.; Lai, Z. P.; Han, Y.; Shi, Z.; Feng, S. H.; Li, J. *Angew. Chem., Int. Ed.* **2012**, *51*, 1412. (c) Cui, P.; Ma, Y. G.; Li, H. H.; Zhao, B.; Li, J. R.; Cheng, P.; Balbuena, P. B.; Zhou, H. C. *J. Am. Chem. Soc.* **2012**, *134*, 18892.

(8) (a) McDonald, T. M.; Lee, W. R.; Mason, J. A.; Wiers, B. M.; Hong, C. S.; Long, J. R. *J. Am. Chem. Soc.* **2012**, *134*, 7056. (b) Arstad, B.; Fjellvag, H.; Kongshaug, K. O.; Swang, O.; Blom, R. *Adsorption* **2008**, *14*, 755. (c) An, J.; Geib, S. J.; Rosi, N. L. *J. Am. Chem. Soc.* **2010**, *132*, 38. (d) Fracaroli, A. M.; Furukawa, H.; Suzuki, M.; Dodd, M.; Okajima, S.; Gandara, F.; Reimer, J. A.; Yaghi, O. M. *J. Am. Chem. Soc.* **2014**, *136*, 8863.

(9) Nguyen, N. T. T.; Furukawa, H.; Gandara, F.; Nguyen, H. T.; Cordova, K. E.; Yaghi, O. M. *Angew. Chem., Int. Ed.* **2014**, *53*, 10645.

(10) (a) Babarao, R.; Jiang, J. W. *Energy Environ. Sci.* **2009**, *2*, 1088. (b) Yu, J. M.; Balbuena, P. B. *J. Phys. Chem. C* **2013**, *117*, 3383. (c) Kizzie, A. C.; Wong-Foy, A. G.; Matzger, A. J. *Langmuir* **2011**, *27*, 6368.

(11) Low, J. J.; Benin, A. I.; Jakubczak, P.; Abrahamian, J. F.; Faheem, S. A.; Willis, R. R. *J. Am. Chem. Soc.* **2009**, *131*, 15834.

(12) (a) Nugent, P.; Belmabkhout, Y.; Burd, S. D.; Cairns, A. J.; Luebke, R.; Forrest, K.; Pham, T.; Ma, S.; Space, B.; Wojtas, L.; Eddaoudi, M.; Zaworotko, M. J. *Nature* **2013**, *495*, 80. (b) Xiang, S.; He, Y.; Zhang, Z.; Wu, H.; Zhou, W.; Krishna, R.; Chen, B. *Nat. Commun.* **2012**, *3*, 954. (c) Li, J. R.; Yu, J.; Lu, W.; Sun, L. B.; Sculley, J.; Balbuena, P. B.; Zhou, H. C. *Nat. Commun.* **2013**, *4*, 1538. (d) Yang, S.; Lin, X.; Lewis, W.; Suyetin, M.; Bichoutskaia, E.; Parker, J. E.; Tang, C. C.; Allan, D. R.; Rizkallah, P. J.; Hubberstey, P.; Champness, N. R.; Thomas, K. M.; Blake, A. J.; Schroder, M. *Nat. Mater.* **2012**, *11*, 710. (e) Chen, B.; Ma, S.; Zapata, F.; Fronczek, F. R.; Lobkovsky, E. B.; Zhou, H. C. *Inorg. Chem.* **2007**, *46*, 1233.

(13) Zhang, Z. J.; Nguyen, H. T. H.; Miller, S. A.; Ploskonka, A. M.; DeCoste, J. B.; Cohen, S. M. *J. Am. Chem. Soc.* **2016**, *138*, 920.

(14) (a) Uemura, T.; Yanai, N.; Kitagawa, S. *Chem. Soc. Rev.* **2009**, *38*, 1228. (b) Uemura, T.; Hiramatsu, D.; Kubota, Y.; Takata, M.; Kitagawa, S. *Angew. Chem., Int. Ed.* **2007**, *46*, 4987. (c) Uemura, T.; Kitaura, R.; Ohta, Y.; Nagaoka, M.; Kitagawa, S. *Angew. Chem., Int. Ed.* **2006**, *45*, 4112.

(15) (a) Czaja, A. U.; Trukhan, N.; Muller, U. *Chem. Soc. Rev.* **2009**, *38*, 1284. (b) McKinstry, C.; Cathcart, R. J.; Cussen, E. J.; Fletcher, A. J.; Patwardhan, S. V.; Sefcik, J. *Chem. Eng. J.* **2016**, *285*, 718.

(16) (a) Rowsell, J. L. C.; Spencer, E. C.; Eckert, J.; Howard, J. A. K.; Yaghi, O. M. *Science* **2005**, *309*, 1350. (b) Chae, H. K.; Siberio-Perez, D. Y.; Kim, J.; Go, Y.; Eddaoudi, M.; Matzger, A. J.; O'Keeffe, M.; Yaghi, O. M. *Nature* **2004**, *427*, 523.

(17) (a) Guo, P.; Dutta, D.; Wong-Foy, A. G.; Gidley, D. W.; Matzger, A. J. *J. Am. Chem. Soc.* **2015**, *137*, 2651. (b) Zhang, W.; Hu, Y. L.; Ge, J.; Jiang, H. L.; Yu, S. H. *J. Am. Chem. Soc.* **2014**, *136*, 16978.

(18) Hausdorf, S.; Wagler, J.; Mossig, R.; Mertens, F. O. R. L. *J. Phys. Chem. A* **2008**, *112*, 7567.

(19) Feng, X.; Ding, X. S.; Jiang, D. L. *Chem. Soc. Rev.* **2012**, *41*, 6010.

DOI: 10.1021/jacs.6b06051
J. Am. Chem. Soc. 2016, 138, 10100−10103